Geoforensics study

The sample material was prepared and studied at the Department of Geography, Geology and the Environment at Kingston University.

Sample material from the wheel bay surface collected with a plastic spatula had to be discarded due to a non-removable contamination with hydraulic oil. Surface deposits collected with *Sellotape* were recovered by soaking 10 cm-stripes of adhesive tape in a mixture of washing-up liquid and deionised water (18 MΩ) in clean 250 ml plastic bottles placed on an orbital shaker at 100 rpm. After 14 hours the remaining sample material was carefully removed from the tape with a clean plastic spatula. Separated particles were then cleaned with deionised water (18 MΩ), disaggregated in deionised water in an ultrasound bath and gently sieved through nylon sieving cloths with mesh sizes of 20 µm, 63 µm and 255 µm[1]. Size fractions 20-63 µm ("fine") and 63-255 µm ("coarse") were used for the geoforensics study. Particles larger than 255 µm were not present in the samples. Each size fraction was split in half and stored in deionised water in a fridge at 5°C to avoid fungi and mould growth or freeze-dried for 16 hours and sputter-coated with gold respectively. Optical analyses were conducted via transmitted light microscopy using a Nikon stereo microscope SMZ1500 equipped with a DS-Fi1 5.24-megapixel digital camera and a Digital Sight DS-US controller using the NIS Elements software for image processing. Clean plastic pipettes were used to transfer the hydrated sample material into clean Petri dishes prior to the optical analysis. High resolution secondary electron (SE) images of the dried and gold-coated sample splits were generated with a Zeiss EVO50 scanning electron microscope (SEM) using a beam current of 100 pA and an acceleration voltage of 5 kV.

The findings of the geoforensics study can be differentiated into three categories: (1) Organic biological substances, (2) inorganic mineralogical substances and (3) anthropogenic industrial substances.

(1) Organic biological matter

A simple assemblage of tree and flower pollen represents the recovered organic matter which is confined to the "fine" size fraction (20-63 µm; Figure 1). The observed pollen grain characteristics are summarised in Table 1. Bisaccate pine tree pollen (family *Pinaceae*, genus *Pinus*) consist of a central pollen body (corpus) and two laterally-placed, chambered sacs (sacci, Figure 2). Total lengths (corpus plus sacci) vary between 60 µm and 100 µm. The air-filled sacci, hollow projections from the corpus, increase the surface area and lower air resistance which facilitates prolonged airborne transport and efficient dispersion. The cappa region on the proximal corpus side has a coarse surface (verrucate ornamentation) while the

1 1000 micrometre (µm) equal 1 millimetre (mm). For comparison, the thickness of human hair can vary between 20 µm and 180 µm depending on hair structure, colour, age, genetic makeup etc.

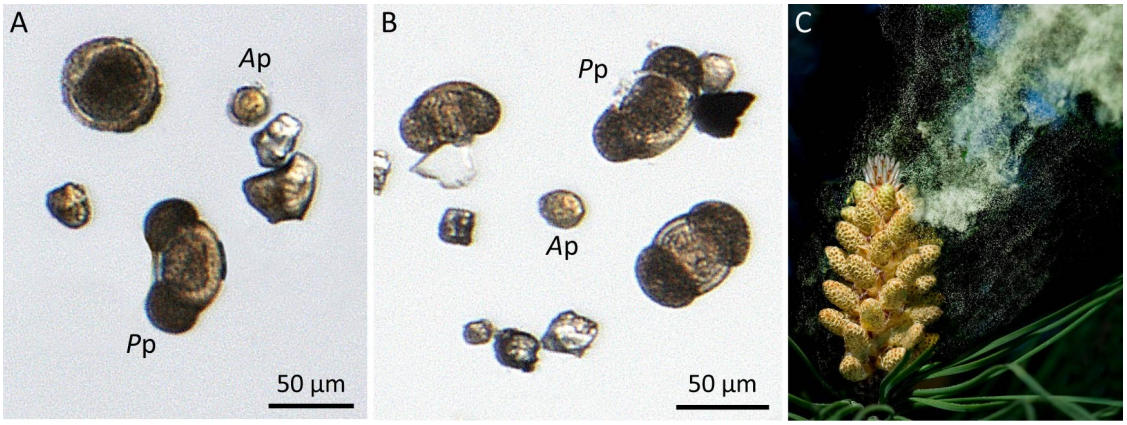

Figure 1. Tree and flower pollen in the “fine” size fraction (20-63 µm). A and B) Transmitted light photomicrographs (plane polarised light) showing *Pinus* (*P*p) and Asteraceae (*A*p) pollen together with fragments of bright-coloured transparent (felsic) minerals. C) Pollen cloud released from a pine cone (ConsciousLifestyle Magazine, 2019).

sacci have smooth surfaces. Discrimination down to species level is difficult due to the morphological resemblance between the numerous native and invasive species in Europe. The Scots Pine (*Pinus sylvestris*) is the only native conifer in the UK and a potential candidate for the observed pine tree pollen grains. Members of the Podocarpaceae family, which are largely restricted to the Southern Hemisphere, can be excluded since they are not common on the Arabian Peninsula (assuming that 777-200LR A6-LRC operated frequently in the Persian Gulf region).

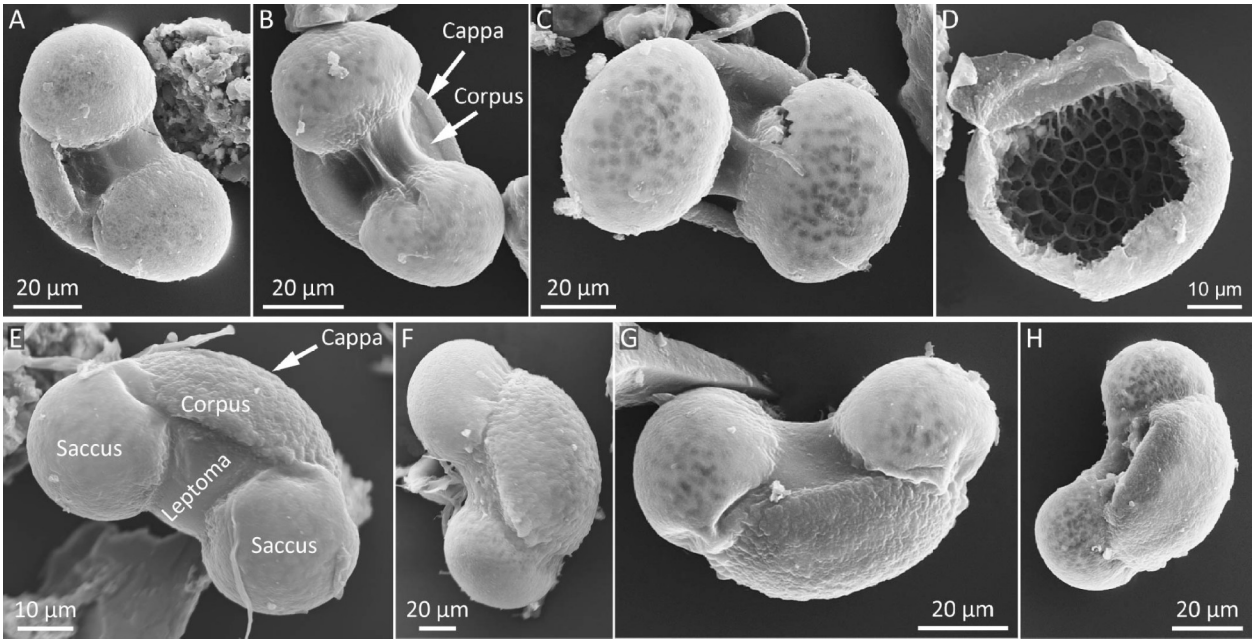

Figure 2. Scanning electron microscope micrographs (secondary electron images) of *Pinus* pollen grains in the “fine” fraction (20-63 µm) of the separated sample material. A-C) Polar distal view. D) Inside of a detached saccus. Note the hexagonal-shaped air chambers. E-H) Straight to oblique equatorial view on fresh hydrated pollen grains illustrating characteristic morphological features.

Table 1. Summary of the observed pollen characteristics.

	Pinus (genus)	**Asteraceae** (family)
Unit	Monad[a]	Monad[a]
Class	Saccate	Colporate
Polarity	Heteropolar[b]	Isopolar[c]
Shape	Bisaccate	Spheroidal
Size (pollen unit)	Large (50–100 µm)	Small to medium (10-50 µm)
Aperture type	Leptoma[d]	Colporate[e]
Ornamentation	Verrucate[f] (cappa)	Echinate[g]

Explanations: [a]Single pollen grain, [b]proximal and distal halves are different, [c]identical proximal and distal poles, [d]thinning of pollen wall at distal pole, presumably the germination area, [e]elongated colpus (ektoaperture) combined with porus (endoaperture), [f]wart-like elements on pollen wall more larger 1 µm, broader than higher (pl. verrucae, [g]spine-like ornamentation element on pollen wall longer or wider than 1 µm (pl. echini).

Spheroidal Asteraceae pollen (composite, aster, daisy or sunflower family) with diameters between 15 µm and 20 µm represent the second, subordinate type of biological matter in the collected samples (Table 1 and Figure 3). The modal proportion between Pinaceae and Asteraceae is approximately 10:1. Pollen walls are densely covered with needle-like elements larger than 1 µm (echini) and contain a single elongated colpus as ektoaperture (Figure 3). A species identification is not possible with the collected data due to the large number of eligible candidates. The composite family of the flowering plants (Angiospermae) includes herbaceous plants (herbs, flowers, weeds) and some woody plants (shrubs, vines, trees) such as the sunflower, lettuce, chamomile, tarragon, chrysanthemum, dandelion and thistle. Asteraceae are endemic to the Northern and Southern Hemisphere, populate all climate zones, have a high biodiversity in Europe and many species are invasive (introduced by human activity; Funk et al., 2019).

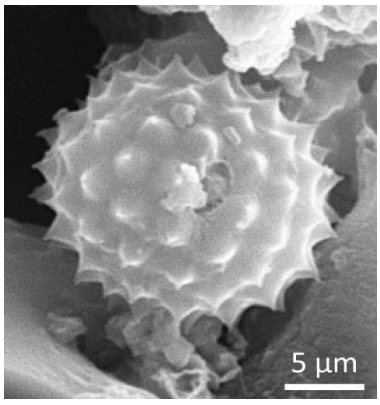

Figure 3. Secondary electron image (SEM) of a medium-sized colporate Asteraceae pollen grain with echinate ornamentation and colpus (ektoaperture).

The limitations of the applied sampling and separation methods (small surface area, low sample depth, material <20 µm not analysed) make it difficult to affiliate the identified pollen material with a specific geographic location or to reconstruct dispersion and migration paths. Airborne

pollen can be transported over long distances upon release (e.g. Smith et al., 2005; Makra and Pálfi, 2007; Skjøth et al., 2007; Rousseau et al., 2008; Izquierdo et al., 2010). Their deposition on a location-independent vehicle is controlled by multiple factors such as local or regional flora, wind patterns, localised (artificial) air turbulences, residence time, exposure etc. The absence of taxa which are endemic to habitats around the Persian Gulf (e.g. halophytes or xerophytes) points to a predominant pollen provenance in the vicinity of the last layover and/or compound site, despite the described sampling biases.

(2) Inorganic mineralogical substances

Light and dark coloured minerals comprise the inorganic particles of natural origin in both separated size fractions (Figure 4). The mineral matter is preserved as complete or fragmented crystals with vitreous lustre and angular to rounded shapes of low to medium sphericity. Mineral surfaces are smooth or scratched, cracked, pitted, porous or frosted as a result of physical and/ or chemical abrasion (Figure 5). Grain sizes range from medium-coarse silt (15.6 µm to 63 µm) to very fine and medium sand (>63 µm to 500 µm) with a predominance of coarse silt to very fine sand particles between 30 µm and 100 µm[2] (Figure 6).

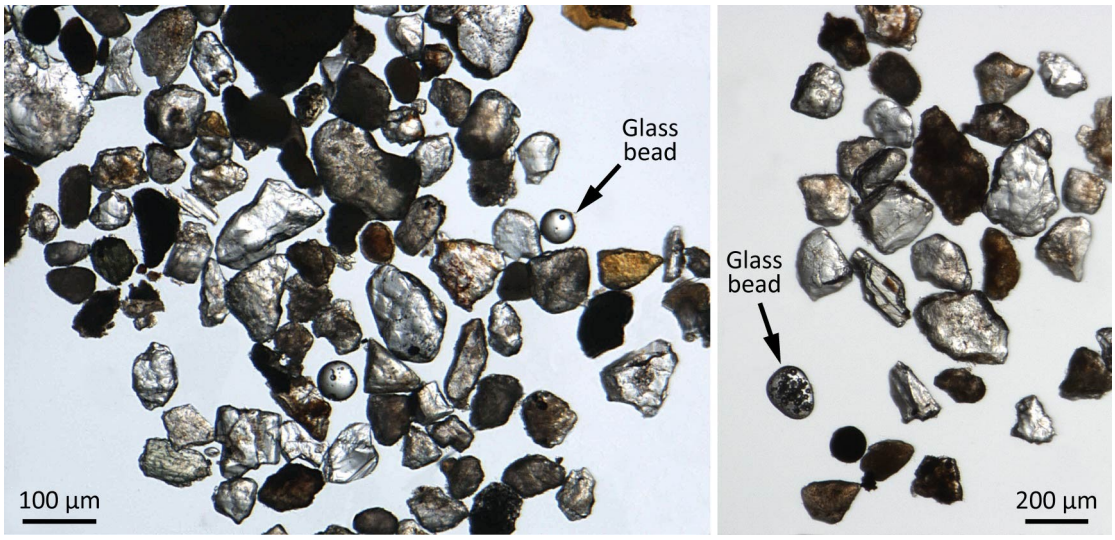

Figure 4. Transmitted light photomicrographs (plane polarised light) showing predominantly angular to sub-angular, felsic (bright) and mafic (dark) mineral fragments in the 63-255 µm-fraction, together with spherical to oval shaped glass beads.

Crystallographic-mineralogical and optical characteristics identify the inorganic particles as predominantly felsic (light coloured) silicate minerals with minor mafic (dark coloured) silicates plus iron oxides and iron oxide-hydroxides. The latter are common weathering and alteration products of primary iron-bearing minerals or of men-made steel products (rust). Quartz (SiO_2)

2 According to the Udden-Wentworth grain-size scale for siliciclastic sediments (Wentworth, 1922). Note that the technical term *sand* does not refer to the composition of a sediment but to the dominate particle size.

and feldspars ((K,Na)[$AlSi_3O_8$] and (Na,Ca)[Al_{1-2},$Si_{2-3}O_8$]) are the dominant felsic minerals in both size fractions. Felsic silicate minerals (from **fel**dspar and **si**li**c**a) are relative enriched in elements with lower mass numbers (e.g. silicon, aluminium, potassium) and have usually specific densities under 3.0 g/cm^3. The darker mafic (from **ma**gnesium and **f**erri**c** iron) silicates contain more elements with higher mass numbers such as magnesium, iron, calcium and sodium and yield specific densities above 3.0 g/cm^3.

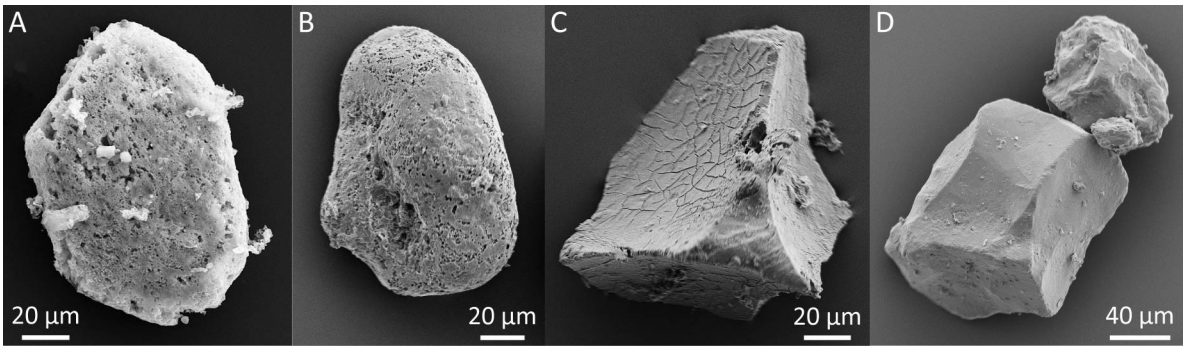

Figure 5. Scanning electron microscope micrographs (secondary electron images) of complete or fragmented minerals in the "coarse" fraction. A) Euhedral (fully-faced) tabular crystal, most likely a feldspar, with frosted-porous surface. B) Anhedral (no external crystal faces) rounded particle with increased sphericity and pitted to porous surface. C) Angular mineral fragment with low sphericity and cracked surface. D) Sub-angular mineral fragment with medium sphericity and smooth surface.

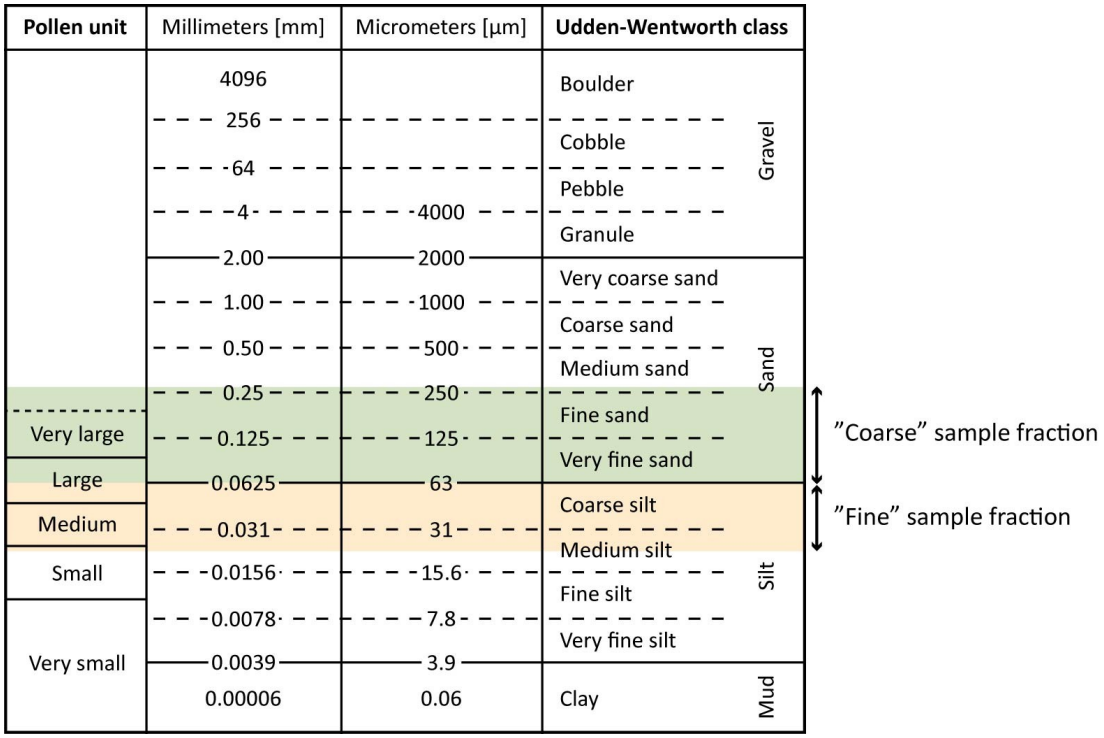

Figure 6. Udden-Wentworth grain-size scale for siliciclastic sediments after Wentworth (1922) and pollen size categories suggested by Hesse et al. (2009). The upper limit of the "Very large" pollen unit is an approximation, based on the largest know pollen sizes (e.g. *Oenothera macrocarpa*, "Missouri evening primrose"). Particle size fractions used for this study are highlighted ("fine": 20-63 µm, "coarse": 63-255 µm).

Silicates are the most important class of rock-forming minerals, accounting for 24% to 27% of the currently valid 5575 mineral species and more than 90% of the Earth's crust (Klein and Hurlbut, 1999; Athena Mineralogy, 2020; International Mineralogical Association, 2020; Webmineral, 2020). Quartz and feldspar minerals are common (felsic) rock-forming minerals in the continental crust (e.g. in granite or andesite) and constitute 63 vol.% of the Earth's crust (Ronov and Yaroshevsky, 1969). This makes the 210 × 106 km^2 of continental crust on Earth (41% of the global surface area; Cogley, 1984; Cawood et al., 2013) the main source region for terrigenous sediment material in subaerial processes. The abundance and availability of major rock-forming minerals makes them accessible for natural mobilisation, transportation and (re-) deposition. The lift force on particles is depended on the flow velocity but also particle features such as size, density, shape and mechanical robustness (hardness). Strong land winds have top speeds around 30 m/s (8 Beaufort) which limits the maximum size of wind-driven aeolian[3] material to medium sand (250-500 µm), creating a natural sorting effect (Pye, 1987; Nickling, 1994). Increased particle roundness, frosted or pitted grain surfaces and compositional maturation (dominance of mechanical robust minerals such as quartz) are characteristic for aeolian sediments and indicative of prolonged airborne transport. Anthropogenic processes such as traffic-related air turbulences interfere locally with natural sedimentation processes on and close to surface level in areas with infrastructure. This has an effect on the nature and composition of airborne particles in proximity to transportation hubs. An additional (complicating) factor is the omnipresence of mineral construction material and waste in agglomerations. This makes is difficult to identify the sediment particle provenance in this study with absolute certainty. Nature and composition of the recovered mineral material speak against an "exotic" origin of the observed mineral particles. The maximum particle size is conform with existing models for wind-driven (aeolian) sediment transport and deposition. Mineralogical composition and particle texture, however, speak against a prolonged airborne transport typical for dune sands on the Arabian Peninsula. Another indicator is the absence of evaporite minerals (carbonates, sulphates and halides such as calcite, anhydrite, gypsum and halite) which are common in supra-tidal mud- and sand flats in semi-arid to arid areas, called sabkhas. Type locations for sabkhas are the coastal low lands of the southern Persian Gulf in the United Arab Emirates, the former operational hub of 777-200LR A6-LRC. Possible provenance areas for the recovered mineral material are the last layover and/or compound sites and their environs.

3 The term derives from Aeolus (Modern Greek Αίολος: "easy to use", "agile", fast moving"), king of the floating island of Aeolia, keeper of the winds by order of Zeus and benefactor of Odysseus, King of Ithaca, in Homer's *Odyssey.*

(3) Anthropogenic industrial substances

Spheroidal to oval, colourless-transparent glass beads with diameters between 35 µm and 100 µm are the only inorganic sample material which is unequivocally anthropogenic in nature (Figure 7). Unspecified iron oxides and iron oxide-hydroxides are either fragments of altered mafic minerals or of men-made steel products. The measured bead diameters (n = 38) cluster around 35 µm, 50 µm, 60 µm, 75 µm and 100 µm which is indicative of standardised size fractions. All glass beads have smooth surfaces and are not coated. Most of the observed glass spheres (ca. 70%) are solid, some are hollow with circular holes (10-25 µm in diameter depending of bead size) and/or contain gas (air) bubbles (Figure 7A, B and D).

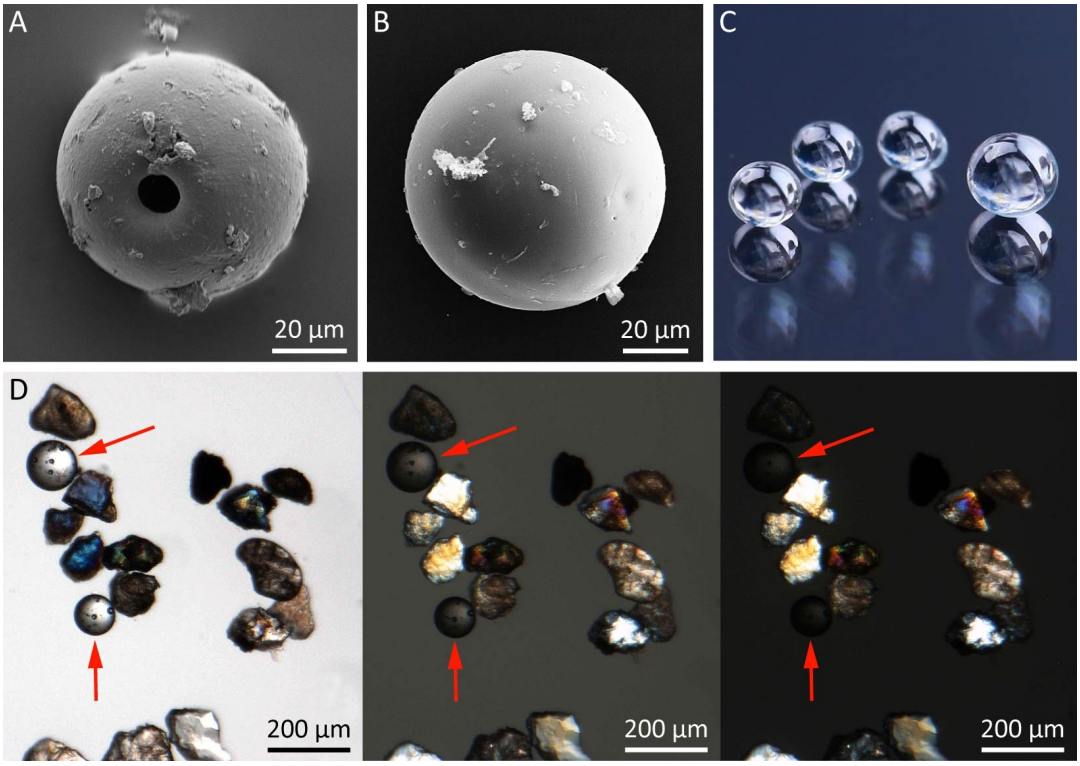

Figure 7. Industrial glass beads in the recovered sample material. A and B) Secondary (SEM-SE) images of hollow (A) and solid (B) spherical glass beads in the “coarse” size fraction. C) Glass microspheres for road marking and traffic paint (Anhui Tory Material Technology Inc., 2020). D) Transmitted light photomicrographs of glass beads (red arrows), felsic and mafic minerals in cross polarised light in three different polariser-analyser alignments. Mineral matter (with a crystal lattice) reveals varying birefringence colours while amorphous glass remains dark.

Glass beads have many technical application across a wide range of industries such as oil and gas, chemicals, construction materials, aerospace, building products, construction and engineering, electrical equipment, machinery, airlines, marine, road and rail, transportation infrastructure, auto components, automobiles, household durables, electronic equipment, instruments and components, electric and water utilities (following the Global Industry Classification Standard; S&P Global, 2020). Their addition to or use as polymers, resins, coatings, abrasives, filtration media, concrete and paints improves material properties such as

thermal and acoustic insulation, friction, hardness, mechanical and chemical resilience, lubrication, light diffusion, light refraction, dispersibility, dimensional homogeneity, adhesion, fluidity and separation, to name a few. Commercial bead sizes range from less than 40 µm up to several millimetres are made of soda-lime glass (70-75 wt.% SiO_2, 12-16 wt.% Na_2O, 10-15 wt. % CaO) or borosilicate glass (70-80 wt.% SiO_2, 7-13 wt.% B_2O_3, 4-8 wt.% Na_2O + K_2O, 2-8 wt.% Al_2O_3; Bauccio, 1994; Pfaender, 1996). Soda-lime glass is a cost-efficient commercial commodity used for the production of everyday objects such as bottles, glasses, food containers and windows. Borosilicate glass is mainly used in specialised products with high chemical and thermal stability (e.g. laboratory equipment, lighting, optical systems, semiconductors, cookware etc.). The application in reflective paints for traffic markings (such as airfield runways) as well as surface treatments (e.g. peening and blasting) in the aerospace industry is the most plausible explanation for glass beads in the sample material (Figure 8). The observed glass bead properties characterise a variegated assemblage of different bead types with differing purposes. Origin and producer of the glass beads remain enigmatic due to the global distribution and use of the product.

Figure 8. Industrial use of glass beads in reflective paint for airfield markings (AviationPros, 2012; Hi-Lite Airfield Services, 2019).

Industrial glass beads are considered an ecologically friendly material which is to some extent reusable in closed surface-treatment systems and in recycling schemes. However, a large proportion of the material enters the natural environment as poorly or non-decomposable solid waste. The physico-chemical and thermal properties make glass inert and stable towards natural decay processes and preserves it in natural systems as anthropogenic matter over thousand to millions of years. The smallest commercially sold glass bead fractions represent respirable health-damaging particles according to the currently valid *WHO Air quality guidelines*. The World Health Organisation (2020) defines atmospheric particulate matter (PM) as solid and liquid substances of organic and inorganic origin which are suspended in the air. The health hazard depends on penetration depth and therewith on particle size. Coarse particulate matter

(PM_{10}) with aerodynamic particle diameters ≤ 10 µm can invade deeper parts of the respiratory system while fine particulate matter ($PM_{2.5,}$ ≤ 2.5 µm) may even cross the barrier into the circulatory system. The overall health risk induced by PM_{10}- to $PM_{2.5}$-sized glass beads remains, nevertheless, minimal considering their localised mobilisation and density in and around airfields or flight paths.

15th June 2020

Dr Andreas Hahn **Date**

Contact:
Dr Andreas Hahn
Department of Geography, Geology and the Environment
School of Engineering and the Environment
Kingston University London
Penrhyn Road
Kingston upon Thames
Surrey KT1 2EE
Email: a.hahn@kingston.ac.uk

References

Athena Mineralogy. (2020) *MINERAL: Silicates. Minerals of class VIII: SILICATES, nesosilicates, sorosilicates, unclassified silicates, cyclosilicates, inosilicates, phyllosilicates, tectosilicates.* [Online] Available from: http://athena.unige.ch/athena/mineral/minppcl8.html [Accessed 11th May 2020].

Anhui Tory Material Technology Inc. (2020) *6088B Glass Microspheres For Road Markings & Traffic Paint*. [Online] Available from: http://cntory.com/6088b-glass-microspheres-for-road-marking-traffic-paint_p15.html [Accessed 5th May 2020].

AviationPros. (2020) *Glass Beads*. [Online] Available from: https://www.aviationpros.com/aoa/runway-managment/product/10133110/flexolite-glass-beads [Accessed 5th May 2020].

Bauccio, M. L. (1994) *Engineering Materials Reference Book.* 2nd edition, Materials Park, OH/USA, ASM International.

Cawood, P. A., Hawkesworth, C. J. & Dhuime, B. (2013) The continental record and the generation of continental crust. *GSA Bulletin*, 125 (1/2), 14-32.

Cogley, J. G. (1984) Continental margins and the extent and number of the continents. *Reviews of Geophysics*, 22, 101-122.

ConsciousLifestyle Magazine. (2019) *Superfood From the Trees: The Incredible Health Benefits of Pine Pollen*. [Online] Available from: https://www.consciouslifestylemag.com/pine-pollen-health-benefits/ [Accessed 13th May 2020].

Funk, V. A., Susanna, A., Stuessy, T. F. & Bayer, R. J. (2009) *Systematics, Evolution, and Biogeography of Compositae*. Wien, International Association for Plant Taxonomy.

Hesse, M., Halbritter, H., Zetter, R., Weber, M., Buchner, R., Frosch-Radivo, A. & Ulrich, S. (2009) *Pollen Terminology - An illustrated handbook*. Wien, Springer.

Hi-Lite Airfield Services. (2019) *Runway Painting*. [Online] Available from: https://www.hi-lite.com/services/airport-markings/21-runway-painting [Accessed 5th May 2020].

International Mineralogical Association. (2020) *Updated list of IMA-approved minerals (March 2020)*. [Online] Available from: http://cnmnc.main.jp [Accessed 11th May 2020].

Izquierdo, R., Belmonte, J., Avila, A., Alarćon, M., Cuevas, E. & Alonso-Pérez, S. (2011) Source areas and long-range transport of pollen from continental land to Tenerife (Canary Islands). *International Journal of Biometeorology*, 66 (1), 67-85.

Klein, C. & Hurlbut Jr., C. S. (1999) *Manual of mineralogy*. New York, John Wiley & Sons Inc.

Makra, L. & Pálfi, S. (2007) Intra-regional and long-range ragweed pollen transport over Southern Hungary. *Acta Climatologica et Chorologica,* 40-41, 69–77.

Nickling, W. G. (1994) Aeolian sediment transport and deposition. In: Pye, K. (ed.) *Sediment Transport and Depositional Processes.* Oxford, Blackwell Scientific Publications.

Pfaender, H. G. (1996) *Schott Guide to Glass*. London, Chapman & Hall.

Pye, K. (1987) *Aeolian Dust and Dust Deposits*. London, Academic Press.

Ronov, A. B. (1969) Chemical composition of the Earth's crust. *American Geophysical Union Monograph,* 13, 50.

Rousseau, D.-D., Schevin, P., Ferrier, J., Jolly, D., Andreasen, T., Ascanius, S. E., Hendriksen, S.-E. & Poulsen, U. (2008) Long distance pollen transport from North America to Greenland in spring. *Journal of Geophysical Research,* 113, G02013.

Skjøth, C. A., Sommer, J., Stach, A., Smith, M. & Brandt, J. 2007. The long-range transport of birch (Betula) pollen from Poland and Germany causes significant pre-season concentrations in Denmark. *Clinical and Experimental Allergy*, 37 (8), 1204–1212.

Smith, M., Emberlin, J. & Kress, A. (2005). Examining high magnitude grass pollen episodes at Worcester, United Kingdom, using back-trajectory analysis. *Aerobiologia*, 21 (2), 85-94.

S&P Global. (2020) *GICS® Global Industry Classification Standard*. [Online] Available from: https://www.spglobal.com/marketintelligence/en/documents/112727-gics-mapbook_2018_v3_letter_digitalspreads.pdf [Accessed 2nd May 2020].

Webmineral. (2020) *Nickel-Strunz Classification (All minerals)*. [Online] Available from: http://webmineral.com/strunz/strunz.php#.Xt_leC2ZPBI [Accessed 11th May 2020].

Wentworth, C. K. (1922) A scale of grade and class terms for clastic sediments. *Journal of Geology*, 30, 377-392.

World Health Organisation. (2020) *Ambient (outdoor) air pollution*. [Online] Available from: http://www.who.int/news-room/fact-sheets/detail/ambient-(outdoor)-air-quality-and-health [Accessed 6th April 2020].